Miscibility and Properties of Semi-Interpenetrating Polymer Networks Based on Polyurethane and Nitroguar Gum

Yihong Huang, Qingchun Fan, Chaobo Xiao

Department of Polymer Science, College of Chemistry and Molecular Sciences, Wuhan University, Wuhan 430072, People's Republic of China

Received 22 November 2005; accepted 17 October 2006
DOI 10.1002/app.25686
Published online in Wiley InterScience (www.interscience.wiley.com).

ABSTRACT: Films from castor oil-based polyurethane (PU) prepolymer and nitroguar gum (NGG) with different contents (10–70 wt %) were prepared through solution casting method. The networks of PU crosslinked with 1,4-butanediol were interpenetrated by linear NGG to form semi-interpenetrating polymer networks (semi-IPNs) in the blend films. The miscibility, morphology, and properties of the semi-IPNs coded as PUNG films were investigated with Fourier transform infrared spectroscopy, scanning electron microscopy, differential scanning calorimetry, dynamic mechanical thermal analysis, wide-angle X-ray diffraction, density measurement, ultraviolet spectroscopy, thermogravimetric analysis, tensile, and solvent-resistance testing. The results revealed that the semi-IPNs films have good miscibility over the entire composition ratio of PU to NGG under study. The occurrence of hydrogen-bonding interaction between PU and NGG played a key role in improvement of the material performance. Compared with the pure PU film, the PUNG films exhibited higher values of tensile strength (11.7–28.4 MPa). Meanwhile, incorporating NGG into the PU networks led to an improvement of thermal stability and better solvent-resistance of the resulting materials. J Appl Polym Sci 104, 4068–4079, 2007

Key words: polyurethanes; guar gum; semi-interpenetrating networks; miscibility; properties

INTRODUCTION

Biodegradable polymers from renewable resources are very actively being researched and developed because of concerns related to the environmental pollution of nondegradable plastic wastes and the great importance of sustainable development.[1,2] Consequently, natural polymers and their derivatives have attracted considerable attention. Among the several candidates including natural polymers and their derivatives, guar gum (GG), a high-molecular weight water-soluble nonionic natural polysaccharide isolated from the seed endosperm of the guar plant, is one of the promising materials for biodegradable plastics because it is a versatile biopolymer with immense potential and low price for use in the nonfood industries.[3] It is a member of the class of galactomannans, which consist of a (1-4)-linked β-D-mannopyranosyl backbone partially substituted at O-6 with α-D-galactopyranosyl side groups.[4] Because of these associations, GG is widely used in food,[5] personal care,[6] and oil recovery. However, the high water sensitivity and bad form-films ability of GG and its derivatives limit their applications as useful film materials. At present there exists several different ways to overcome these problems, one of them is mixtures of synthetic polymers with natural polymers (preparation of polymer mixtures) which have good biodegradable properties; another option is the synthesis of polymers with use of products from natural sources.[7]

In past decades, polymer blends continue to be a subject of intensive investigations in both industrial and academic domains because of the simplicity and effectiveness of mixing two different polymers to obtain new materials.[8] Especially, the development of composite materials using renewable resources which are naturally biodegradable and the possibility of combining their biodegradability with cost reduction and market needs have been the object of intensive academic and industrial research.[9] Interpenetrating polymer networks are defined as a combination of two polymers in network form, at least one of which is crosslinked in the immediate presence of the other, such as polyurethane (PU) and others.[10] The interpenetrated system resulting from one crosslinked polymer and one linear polymer is considered a semi-interpenetrating polymer networks (semi-IPNs).[11]

PU has been widely used as one of the individual polymers possessing networks structure owing to its good flexibility and elasticity. Nowadays, semi-IPNs materials prepared from castor oil-based PU with natural polymer derivatives have exhibited excellent properties. Gao and Zhang[12,13] firstly reported the

Correspondence to: C. B. Xiao (cbxiao@whu.edu.cn).

interpenetration and entanglement of nitrokonjac glucomannan into PU networks can result in great enhancement of mechanical properties of PU composite materials. Later, Zhang and Huang[14,15] and Lu and Zhang[16] reported the incorporation of natural polymers into PU plays an important role in accelerating curing and enhancing mechanical strengthen of the PU materials. Hence, the semi-IPNs based on castor oil-based PU and natural polymer have a potential application as useful composite materials. More, some authors[17–19] have reported that the semi-IPNs materials can be applied in water-resistance films. For the coated films, the PU prepolymer gives rise to a shared network between materials and the coating compositions, resulting in the strong interfacial bonding interactions. Recently, Zhang et al.[20] and Lu and Zhang[21] have successfully synthesized regenerated cellulose films coated with PU/nitrocellulose and PU/benzyl konjac glucomannan semi-IPNs coating, respectively. This showed that a shared PU network crosslinks simultaneously with cellulose and that semi-IPNs coating occurs in these compound sheets, resulting in the enhancement of mechanical properties and the optical transmittance. More important, the biodegradability of these IPN-coated cellulose films were investigated, and the results indicated that they were degraded by microorganisms in soil, accompanied by the production of CO_2, H_2O, glucose cleaved from cellulose, aromatic ethers from PU, and other products. Hence, the development of semi-IPNs from PU and natural products can stimulate both the utilization of renewable resources and synthesis of biodegradable materials.

In this study, we attempted to prepare novel blend films from castor oil-based PU and nitroguar gum (NGG) with a content of 10–70 wt % in the presence of 1,4-butanediol as a chain-extender agent. In the case, the linear NGG should be interpenetrated into the PU networks to form semi-IPNs. Their structures and morphologies of the semi-IPNs were characterized with Fourier transform infrared spectroscopy (FTIR), scanning electron microscopy (SEM), differential scanning calorimetry (DSC), dynamic mechanical thermal analysis (DMTA), wide-angle X-ray diffraction (WAXD), thermogravimetric analysis (TGA), ultraviolet spectroscopy (UV), density measurement, tensile, and solvent-resistance testing, respectively. The investigation of the effects of NGG content on the miscibility and properties of the semi-IPNs materials may contribute meaningful information for the development of novel biodegradable polysaccharide-based materials.

EXPERIMENTAL

Materials

All the regents were obtained from commercial resources in China. GG was kindly surpplied by Wuhan Tianyuan Biology Industries, China. The method of preparation and purification were followed as described earlier.[22,23] The castor oil was chemically degraded and was dried at 110°C under 20 mmHg for 2 h. Commercial 2, 4-toluene diisocyanate (TDI; Shanghai Chemical, China) was vacuum-dried at 80°C for 2 h and was used as hard segments. 1,4-butanediol (BDO; Shanghai Chemical, China) was used as a chain-extender and crosslinker agent. Tetrahydrofuran (THF) was dried over molecular sieves. The other reagents were used without further purification.

Preparation of NGG

Ten gram of GG was taken in a round-bottomed flask equipped with a mechanical stirrer. The 100 mL fuming nitric acid was poured into the flask and the solution was stirred dramatically at once, then 67 mL acetic anhydride was added by droplet under an ice/salt bath with stirring. The reaction was controlled at room temperature for 4 h. The resulting solution was poured into excess cold water to precipitate NGG. This crude product was dissolved with acetone and then was precipitated and washed several times with water. After vacuum-drying at 50°C, the white powdered NGG was obtained. The elemental analysis of GG and NGG was obtained with a rapid elemental analyzer (Heraeus, Germany). The DS value of NGG was found to be 2.1. The FTIR spectra of GG and NGG are shown in Figure 1. The broad stretching band of —OH groups around 3394 cm^{-1} for GG was sharply decreased in the spectrum of NGG, indicating that the hydrogen atoms of —OH groups in GG were substituted by $—NO_2$ groups. Furthermore, three obvious absorption bands, at 1660, 1283, and 835 cm^{-1}, were assigned to the $—ONO_2$ groups,[24] indicating that NGG had been synthesized successfully. The weight-average molecular weight (M_w) of NGG in THF was determined by Debye plots by using a multi-angle laser photometer equipped with a He–Ne laser (λ = 633 nm; DAWN-DSP, Wyatt Technology, USA). Astra software was utilized for data acquisition and analysis. The M_w of NGG was determined to 2.33×10^5, and its polydispersity (M_w/M_n) was 1.52.

Preparation of PUNG films

Castor oil based-PU prepolymer (NCO/OH = 2, molar ratio) was prepared according to the method described by Sperling.[25] Fifty-seven gram castor oil (4.49 wt % hydroxyl groups, hydroxyl value = 163) was added slowly with stirring to a round-bottom flask with 29 g TDI under a nitrogen atmosphere. The reaction was carried out at 45°C for 2 h to produce the PU prepolymer. Then, 3 g of PU prepolymer was mixed with the desired weight of NGG,

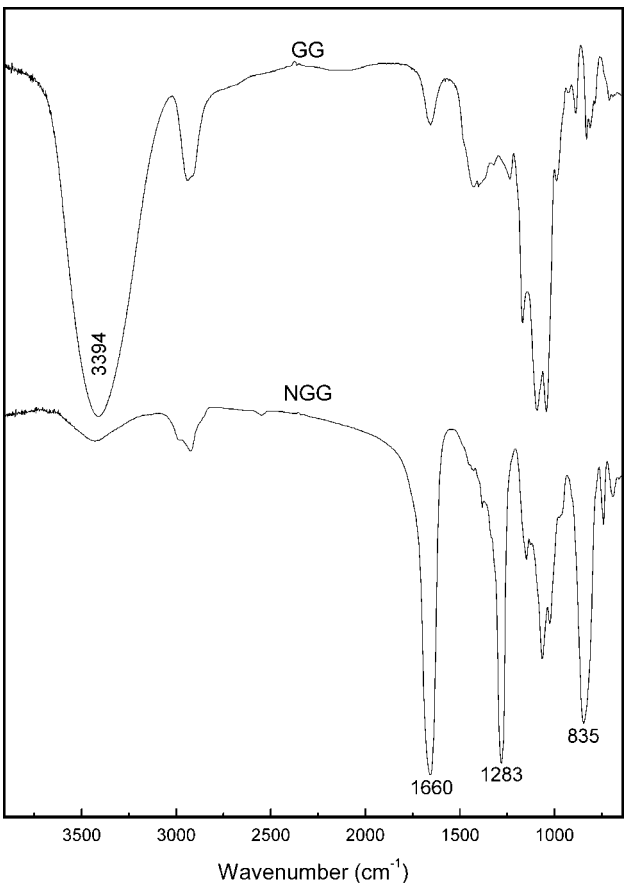

Figure 1 FTIR spectra of guar gum (GG) and nitroguar gum (NGG).

0.45 g of BDO as a chain-extender agent (the amount being adjusted to give total [NCO]/[OH] = 1) in THF at room temperature. The resulting mixture was adjusted by adding THF to make a solid content of 20 wt %. It was then cast on a glass plate and cured at room temperature until there was complete evaporation of the THF solvent, then was moved into an oven in 50°C to form dry film. The thickness of the films was controlled to be about 100 μm. By altering the content of NGG in the films to 0, 10, 20, 30, 40, 50, 60, and 70 wt %, a series of films coded as PU, PUNG-10, PUNG-20, PUNG-30, PUNG-40, PUNG-50, PUNG-60, and PUNG-70 was prepared. The films were vacuum-dried at room temperature for 3 days and kept in a desiccator with P_2O_5 as a desiccant for more than 1 week before the characterization.

Characterization

FTIR spectra of the GG and NGG were recorded with a Nicolet 170SX Fourier transform infrared spectrometer using KBr-pellets, at room temperature. Attenuated total reflection Fourier transform infrared (ATR-FTIR) spectroscopy of the blend films was performed at room temperature on a Nicolet ATR-FTIR spectrometer (Avatar 360, USA) fitted with a germanium crystal, with a fixed 45° angle of incidence. The samples with thickness of about 100 mm were taken at random from sheets and placed flat on the crystal surface. The data were collected over 32 scans with a resolution of 4 cm^{-1}.

DSC thermograms over the temperature range from −30 to 150°C were recorded using a DSC (TA2920, USA) under a nitrogen atmosphere. Samples (15–20 mg) were cut from extruded strands conditioned at 98% RH and analyzed. Each sample was subjected to the heating/cooling cycle between −50 and 200°C to obtain reproducible the glass temperature (T_g) values. For a polymer, T_g was taken at the half-variation in heat capacity occurring at the glass-rubber transition. Scanning rate in the second run was 5°C/min.

DMTA were carried out on a dynamic mechanical thermal analyzer (DMTA-V, Rheometric Scientific, USA) in rectangular tension mode. The temperature program was run from −50 to 200°C using a heating rate of 5°C/min at a fixed frequency of 1 Hz. Square specimens with dimensions of 10 mm ×10 mm were used.

SEM images were taken on a Hitachi S-570 (Japan) microscope. The films were frozen in liquid nitrogen and snapped immediately, and the surface section of the films was puttered with gold, observed, and photographed. For the observation of the semi-IPN structure, the PUNG films, enclosed in a nylon mesh, were immersed in *N,N*-dimethylformamide (DMF), and this was accompanied by mild stirring for 24 h at room temperature; thus, NGG, weakly interacting with PU, was dissolved in DMF and removed from the PU networks during extraction, leaving voids. The extracted films were frozen in liquid nitrogen and snapped immediately, and the surface sections of the films were coated with gold for SEM observations.

WAXD patterns of the films were recorded on D/max-1200 X-ray diffractometer (Rigaku Denki, Japan) with Cu-Kα radiation ($\lambda = 1.5405 \times 10^{-10}$ m), and the samples were examined with 2θ ranging from 8 to 50° at a scanning rate of 4°/min.

TGA thermograms of the specimens were recorded on a thermoanalyzer (DT-40; Shimadzu) under nitrogen atmosphere with a flow capacity of 50 mL/min from 20 to 600°C, at a heating rate of 10°C/min. The corresponding decomposition temperature and weight loss values of the samples were evaluated by using the intersection point of tangents of TGA curves.

The thermal degradation kinetic parameters for the films and NGG were measured from the TGA thermogram using Broido[26] methods, which provides overall kinetic data averaged for the experimental temperature range. For the sake of the calculations and to know the nature of the decomposition,

the complete thermogram was divided into three distinct sections. The activation energy (E) for the thermal degradation processes was evaluated using Broido equation:

$$\ln\left[\ln\left(\frac{1}{y}\right)\right] = -\frac{E}{R}\left(\frac{1}{T}+K\right)$$

where R is the gas constant, T the temperature (in K), K any constant, y the normalized weight (w_t/w_0), w_t denotes the weight of the sample at any time, while w_0 stand for its initial weights, respectively. The energy of activation (E) can be obtained from the plot of $\ln[\ln(1/y)]$ versus $1/T$.

The tensile testing of the films were measured on a universal testing machine (CMT6502, Shenzhen SANS Test Machine, China) with a tensile rate of 5 mm/min according to ISO6239-1986 (E) to obtain tensile strength (σ_b) and breaking elongation (ε_b). The mean values of σ_b and ε_b were obtained from three replications, respectively.

The density (ρ) of the blend films was measured at 25°C by determining the weight of a volume-calibrated psychomotor filled with a mixture of sodium chloride aqueous solution and distilled water, in which the samples achieved floatation level. The density of the liquid mixture equals the density of the samples. Three parallel measurements were carried out for every sample.

The optical transmittance (T_r) of the films was measured with an ultraviolet-visible spectrophotometer (UV-160A, Shimadzu, Japan) at 800 nm.

Solvent-resistance testing of the films was performed with different solvents including distilled water, 20 wt % HCl solution, 20 wt % NaOH solution, 20 wt % NaCl solution, toluene, and ethanol at room temperature for a week. The dry films were weighed and then immersed into the solvent to prepare films for 7 days. The resulting film was taken out, and the excess solvent on the film was wiped off to weigh. The weight loss rate was calculated by the following equation:

$$W_{\text{loss}}\ (\text{wt \%}) = [(w_0 - w_s)/w_0]/100\%$$

where w_s represent the weight of the swollen film and w_0 is the weight of the dry film.

RESULTS AND DISCUSSIONS

Structure and morphology of the blend films

Figure 2 shows the FTIR spectra of the PU and PUNG films, while the corresponding FTIR spectra of the blends in the —NH region (4000–3000 cm^{-1}) and —C=O (2000–1600 cm^{-1}) are also illustrated in Figure 3. It is well known that FTIR spectrometer is a powerful instrument for the investigation of the hydrogen-bonding behavior of PU. For the pure PU film, the NH stretching vibration bands are thought be composed of hydrogen-bonded —NH (3330 cm^{-1}) and free —NH (3438 cm^{-1}), while the —C=O consists of hydrogen-bonded —C=O (1725 cm^{-1}) and free —C=O (1703 cm^{-1}).[27–29] The —NH in PU is mainly hydrogen-bonded with —C=O in hard-segments and the ether-oxygen or ester-oxygen of soft-segments.[30] With NGG content increased, intensity of peak at free —NH increased, while that of peak at hydrogen-bonded —NH decreased in the PUNG films. Moreover, when compared with the pure PU, the —NH stretching vibration exhibited strong absorption and shifted to a higher wavenumber from

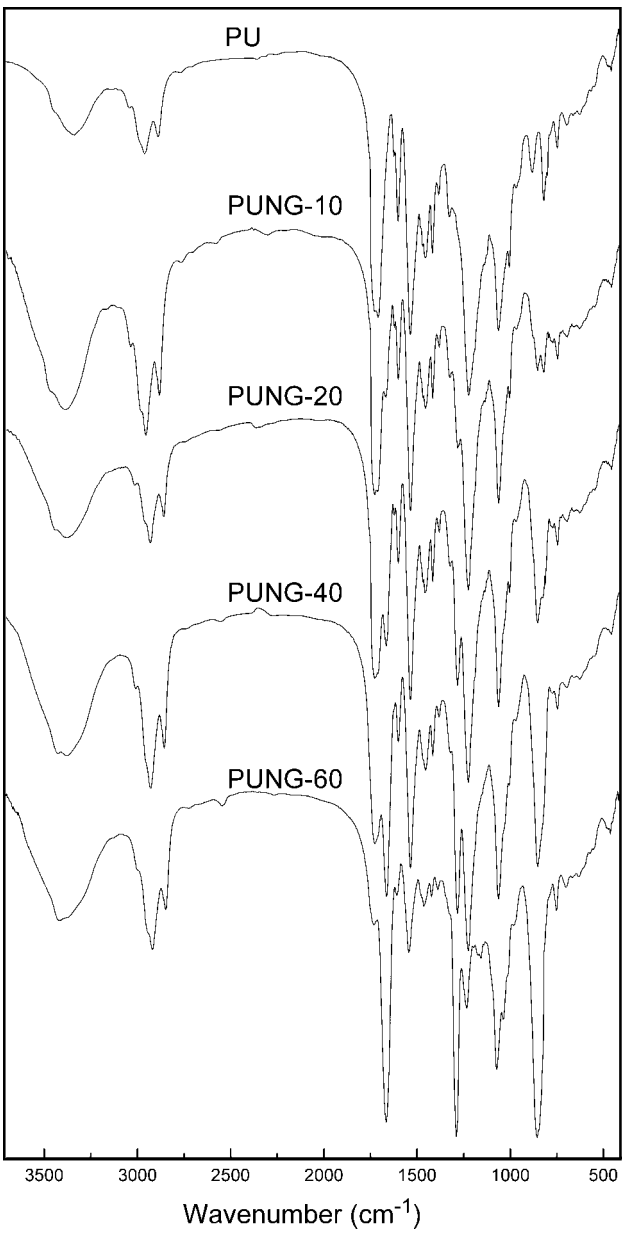

Figure 2 FTIR spectra of the PU and PUNG films.

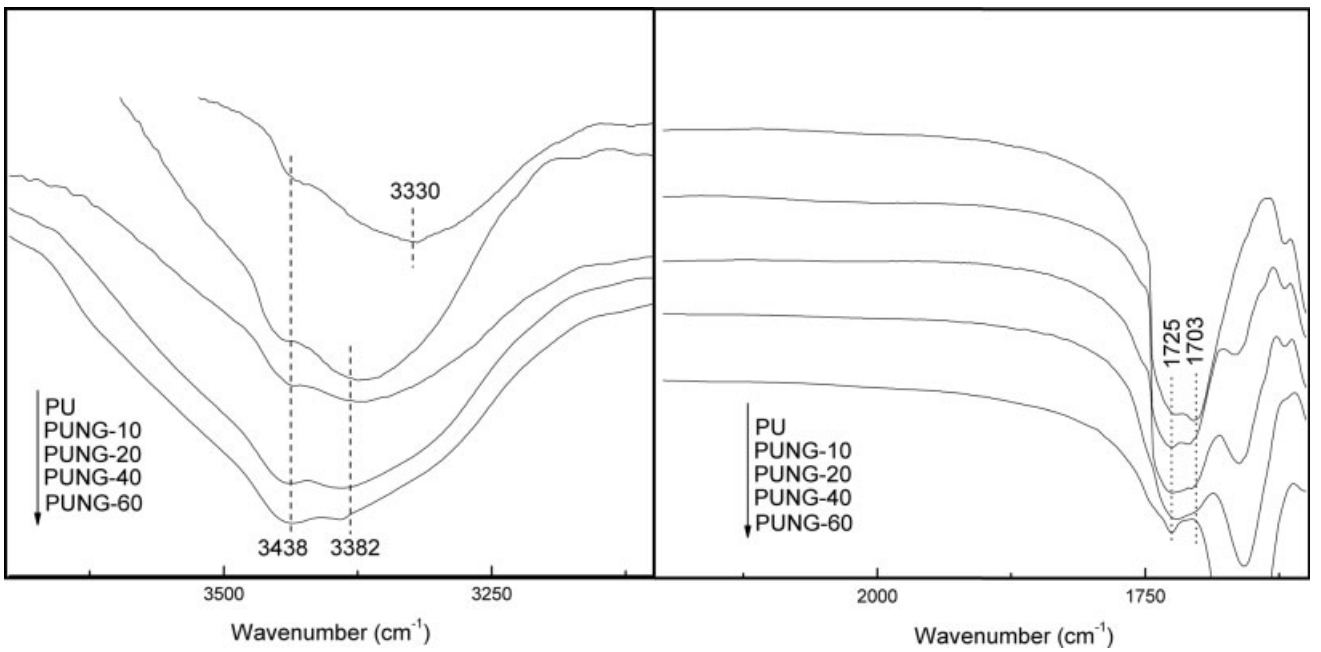

Figure 3 FTIR spectra of the blends in the —NH region (4000–3000 cm^{-1}) and —C=O (2000–1600 cm^{-1}).

3330 to 3382 cm^{-1} with an introducing of NGG. These changes indicated the original intermolecular and intramolecular hydrogen-bonding involved in PU were broken in the semi-IPNs as a result of the interpenetration and entanglements between PU networks and NGG molecules. In the case, —C=O can be hydrogen-bonded with —OH of NGG and BDO or the urethane —NH. The intensity of peak located at 1703 cm^{-1} decreased, while that of peak at 1725 cm^{-1} increased gradually with an increase in the NGG content, which indicated that the fraction of the —C=O hydrogen-bonded with —OH of NGG or BDO increased. The FTIR results suggested that interpenetration between PU and NGG occurred over the whole range of composition ratio of NGG to PU under study, resulting in the formation of a strong intermolecular interaction attributed to hydrogen-bonding in the semi-IPNs structure.

SEM images of surface sections of the NGG, PU, and PUNG films are shown in Figure 4. Except the porous surface in NGG, all of the films showed smooth surface and dense structures without pores or cracks. Even so, the blend films with high NGG content did not show any evidence of phase separation. The homogeneous structure of films was observed, which indicated high compatibility and miscibility between PU and NGG in entirely ratio range under study, and good mechanical properties would be expected. At the same time, SEM images of surface sections of the films extracted with DMF were shown in Figure 5. The PUNG films exhibited homogeneous porous architecture, indicating good miscibility between PU and NGG. There were some voids in the PU matrix, from which the NGG molecules have been removed by DMF. Clearly, the extraction made the free surface coarse and porous, and the degree increased with an increase of NGG content. When NGG content in the PUNG films were lower than 40 wt %, NGG molecules as a dispersed phase were proportionally separated into PU matrix. When the content of NGG increased up to 50 wt %, the dark domain was extended and became a dual-continuity phase. In addition, SEM images of the blend films consists of more high NGG content cannot be obtained because of the difficult preparation of the extracted samples. However, NGG is thought to exist as a continuous phase in PUNG films with relatively high NGG content. Consistent with most cases, the major component of the blend films formed the continuous phase, whereas the minor component formed the dispersed phase without obvious phase separations.

Miscibility between PU and NGG in the blend films

DSC curves of the NGG, PU, and PUNG films are shown in Figure 6, and the corresponding data are detailed in Table I. The changes of T_g in PU system are usually attributed to the microphase mixing between soft-segments and hard-segments and the restriction on rotation of the soft-segment linked to hardsegment.[31] NGG showed no glass transition in the DSC thermograms, but all the PUNG films and pure PU showed glass transition. In addition, no endothermic peaks appeared in the scans, indicating

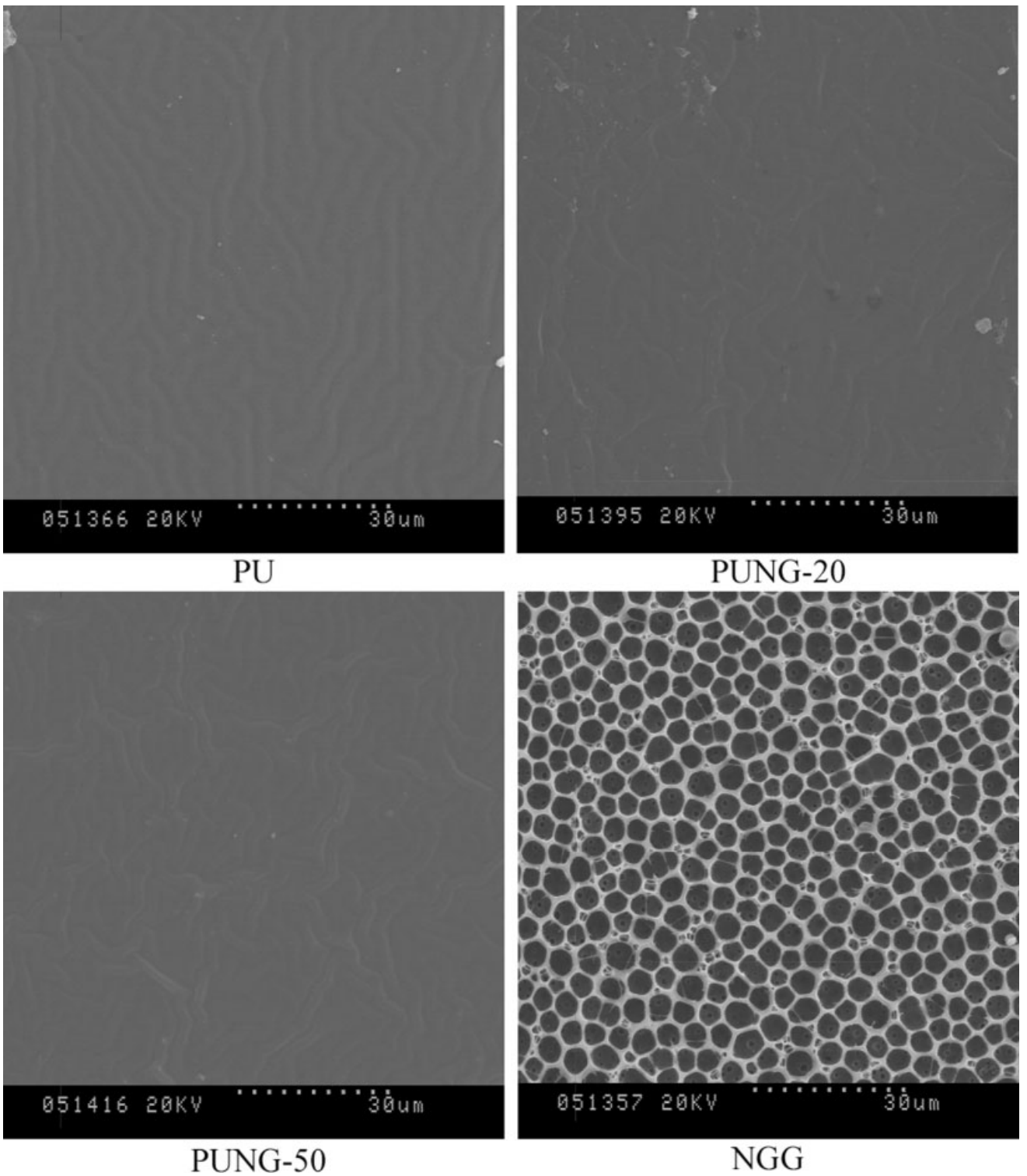

Figure 4 SEM images of surface sections of the PU, PUNG films, and NGG.

that crystalline regions did not exist in our samples. The DSC analysis also showed that the T_g shifted to higher temperatures with an enhancement of NGG content which was explained that the incorporation of stiff NGG component resulted in a decrease in the flexibility and mobility of the PU soft segments. The concentration fluctuation of the PU molecular chain and the restriction of PU molecular motion due to the interaction between two polymers were responsible for the obvious microphase separation between the soft and hard segments of PU.[32]

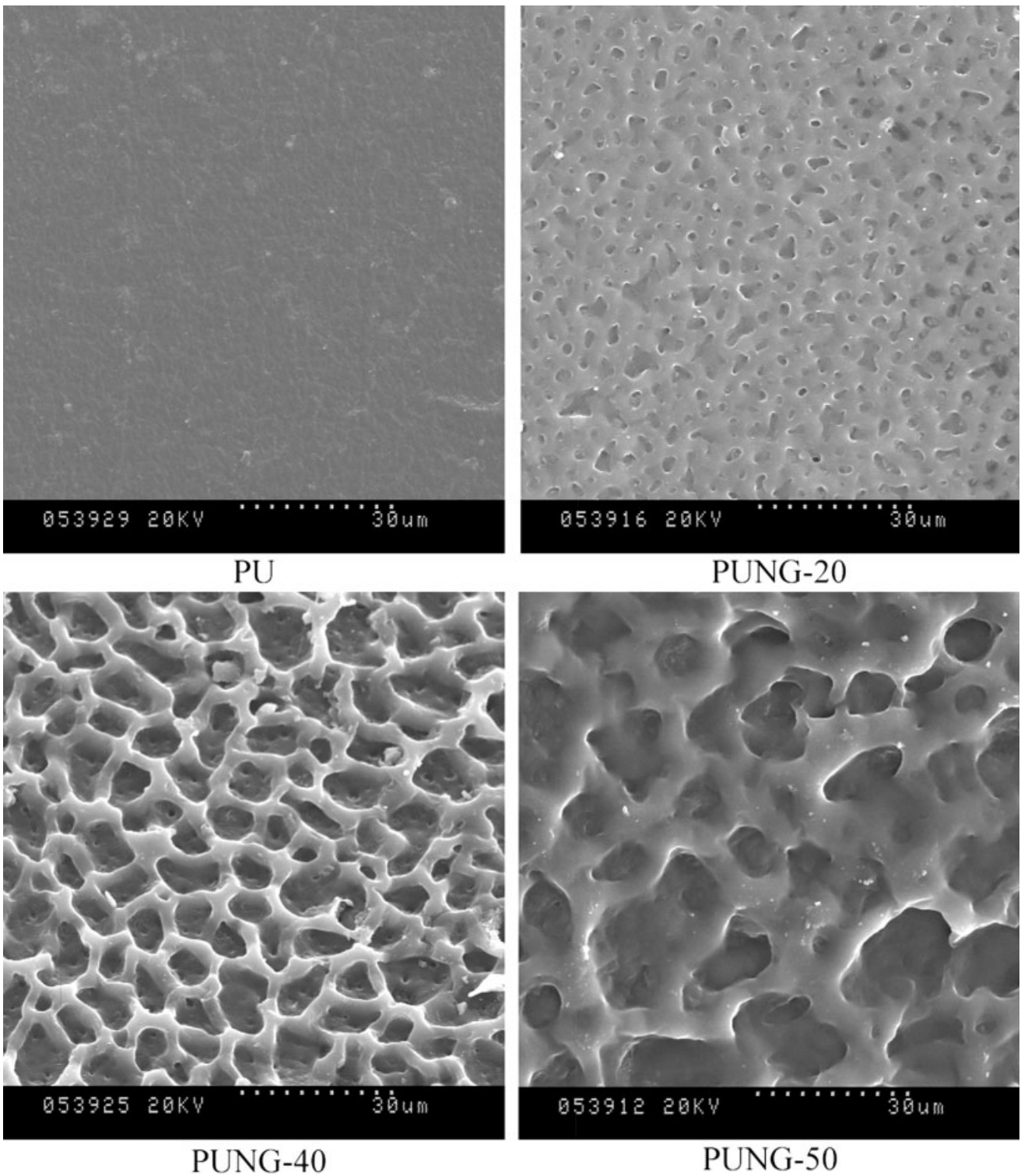

Figure 5 SEM images of surface sections of the PU and PUNG films extracted with DMF.

DMTA can be used to study the miscibility of a polymer blend.[33] Usually, mechanical loss factor (tan δ) peak in the DMTA thermogram, the a-relaxation, reflects the glass transition, and may be analyzed to provide information about the motion of molecules. The T_g obtained from DMTA was higher than that measured by DSC. To illustrate this difference, the nature of DMTA and DSC measurements should be referred. The thermodynamic mechanical relaxation of DMTA results from motion of chain segments, while calorimetry corresponds to a larger scale motion, that is, whole molecules or groups of several

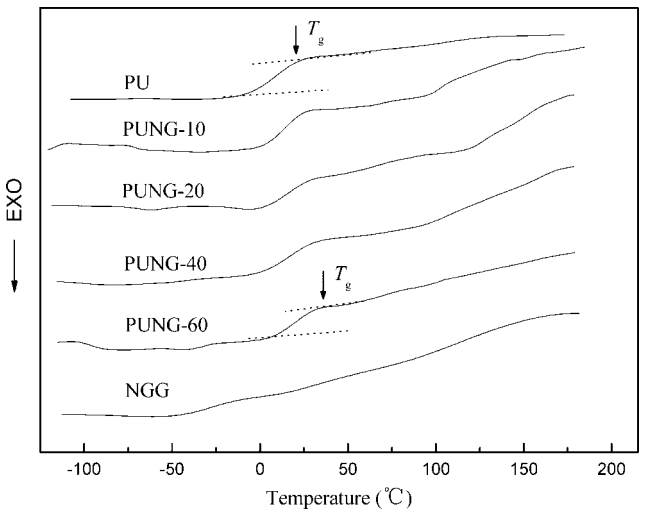

Figure 6 DSC thermograms of the PU, PUNG films, and NGG.

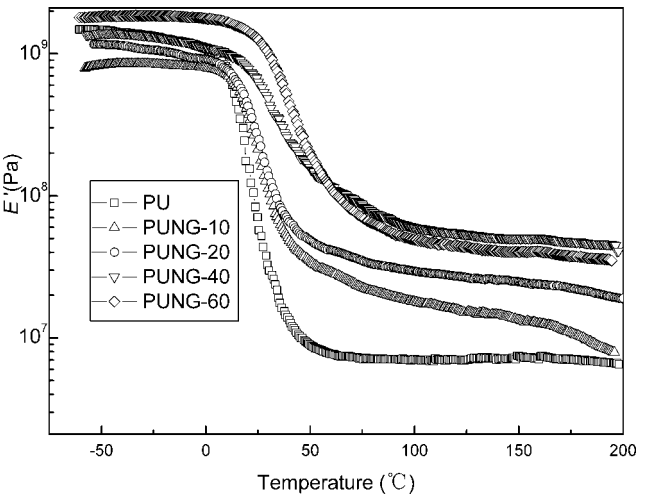

Figure 7 Temperature dependence of E' for the PU and PUNG films.

molecules.[34] Another explanation for the difference is that DMTA measurements reflect the T_g of soft-segment microphase, while DSC measurement records indicate the T_g of pure soft segment.[35]

The storage modulus (E') and mechanical loss factor (tan δ) of the PU and PUNG films as functions of the temperature are plotted in Figures 7 and 8, respectively, and the corresponding data are summarized in Table I. The storage modulus of the PUNG films with NGG content lower than 20 wt % showed a drop in stiffness, accompanying the glass transition (T_g) of the PU soft segments. When the NGG content is higher than 20 wt %, the PUNG films exhibit higher E' values, and this indicated that NGG played a role in toughness reinforcement. In this case, T_g, corresponding to the α-transition, shifted from 22.7 to 43.6°C with an increase in NGG content, and this was in good agreement with the DSC results. The position of the damping peak in the tan δ/temperature curves, which are related to the structure, composition, and crystallization behavior, may reflect the molecular motion and interaction sensitively. Furthermore, the height of the α-relaxation peak can be used to analyze the molecular motion of crosslinking polymers. From a plot of tan δ versus temperature, the height of the damping peaks of PU in the films decreased and the T_g value obviously shifted to higher temperature. Especially, the damping peaks of PU almost disappeared in the PUNG-60 film. The higher T_g value and decreasing height related to PU soft segment was associated with lower segmental mobility, which was explained that the soft segments of PU penetrated into the rigid molecules of NGG and the mobility of soft segment assigned to PU was restricted because of the hardness of the main chain for NGG.

In a polymer blend where no adhesion between the interface and no molecular mixing occur at the phase boundary, the density of the blend films would be expected to follow the rule of mixtures.[16] As a result, the positive deviation of the densities for semi-IPNs materials can be attributed to intimate interpenetration and chain packing, leading to reduction of the free volume. As shown in Figure 9, the

TABLE I
DSC and DMTA Results for PU and PUNG Films with Various NGG Contents

	DMTA		DSC	
Samples	T_g (°C)	Tan δ	T_g (°C)	ΔC_P (J/°C)
PU	22.7	1.05	5.83	0.322
PUNG-10	31.2	0.56	11.4	0.365
PUNG-20	34.6	0.34	14.7	0.336
PUNG-40	41.5	0.23	16.1	0.354
PUNG-60	43.6	0.12	19.5	0.309

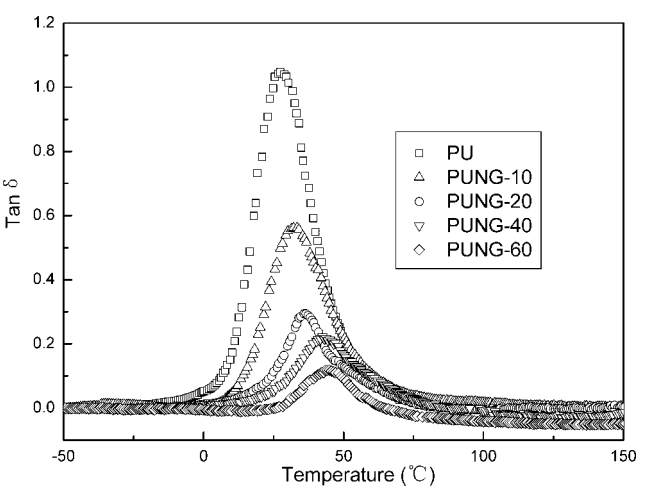

Figure 8 Temperature dependence of tan δ for the PU and PUNG films.

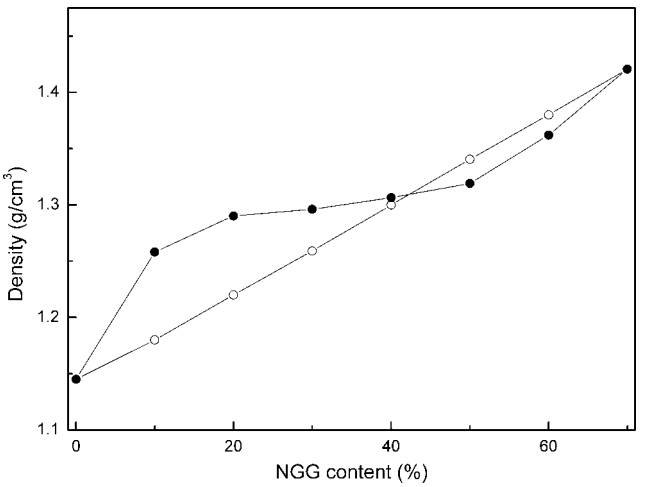

Figure 9 Dependence of the densities on NGG content from theoretical values (○), and experimental values (●) for the PU and PUNG films.

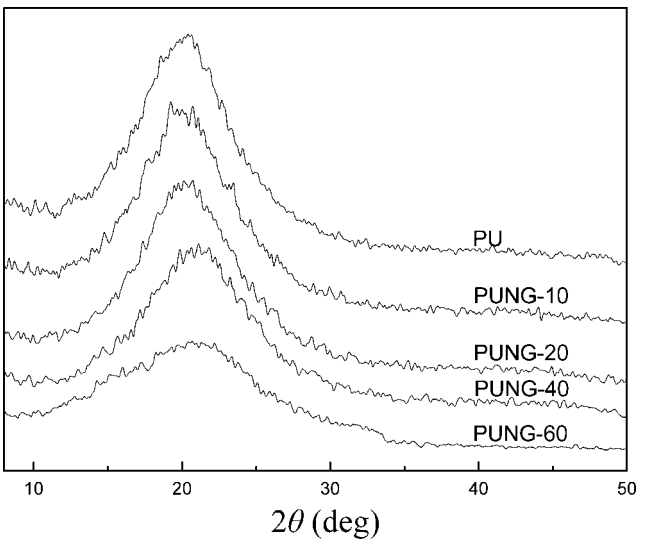

Figure 11 WAXD diffraction patterns of the PU and PUNG films.

PUNG films showed positive density deviations than that from addivity rules for the PUNG films when the NGG content was less than 40 wt %, which indicated that an intimate interpenetration of interchains between PU and NGG led to a reduction of the free volume of original PU in the PUNG films.

The transparency of the films is an auxiliary criterion to judge the miscibility of the composite materials.[36] The interface between the two materials causes losses in T_r of the quantity of light, which is normally scattered and reflected at the interface of different solids.[37] The dependence of optical transmittance (T_r) at 800 nm on NGG content is shown in Figure 10. Interestingly, the PUNG films with NGG content lower than 20 wt % exhibited higher T_r than pure PU film, suggesting there was relatively high compatibility and miscibility between NGG and PU. Enhanced T_r of the films can be explained that adhesion between two kinds of the molecules with small dispersed phase domain was very intimate, and the amorphous state enhanced, because of the semi-IPNs structure.[38]

WXRD patterns of the films are shown in Figure 11. A broad halo commencing from 13 to 32° in 2θ with lower magnitude is found for the pure PU and PUNG films, and the data also does not show clear Bragg diffraction peaks. This indicates the amorphous nature of the PU and PUNG films.

Thermal properties of the blend films

The thermal degradation patterns of the films are shown in Figure 12, and the corresponding data are

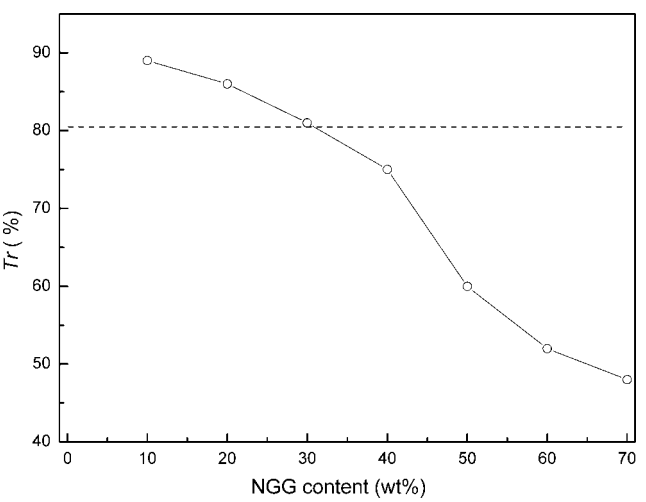

Figure 10 Dependence of optical transmittance (T_r) at 800 nm on NGG content for PUNG films. The dashed line represents the dependence for a PU film at 800 nm.

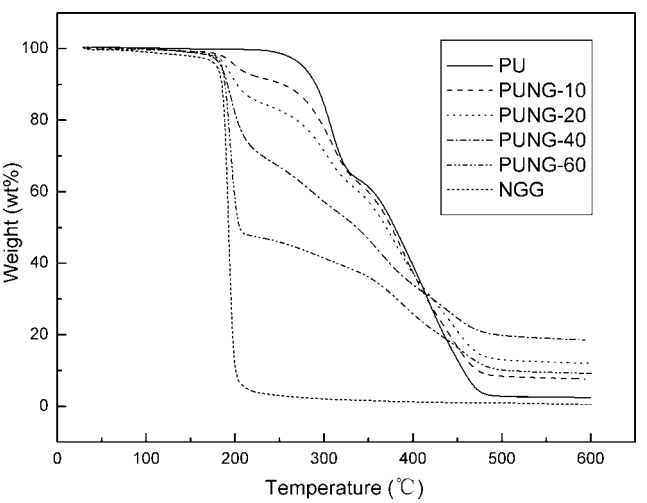

Figure 12 TGA thermograms of the PU, PUNG films, and NGG.

TABLE II
Weight Loss, Activation Energy, and Corresponding Decomposition Temperature for the PU, PUNG Films, and NGG

Samples	Process	Transition range[a]			E (kJ/mol)	Weight loss (%)
		T_i (°C)	T_m (°C)	T_f (°C)		
PU	1	–	–	–	–	–
	2	278	302	321	266.8	32.6
	3	363	408	465	122.7	56.1
PUNG-10	1	184	196	207	241.9	5.2
	2	279	297	325	192.6	22.6
	3	363	404	461	129.5	48.4
PUNG-20	1	181	196	210	246.1	11.9
	2	278	302	321	266.8	32.6
	3	363	408	465	122.7	56.1
PUNG-40	1	184	196	209	252.2	24.9
	2	276	293	317	201.3	15.5
	3	354	402	470	102.9	43.1
PUNG-60	1	182	193	202	315.0	49.8
	2	283	308	327	204.9	4.3
	3	368	421	477	113.7	15.3
NGG	1	184	193	198	372.7	92.9
	2	–	–	–	–	–
	3	–	–	–	–	–

[a] T_i, temperature at which decomposition starts; T_m, temperature at which decomposition rate is maximum; T_f, temperature at which decomposition is completed.

summarized in Table II. Generally, the thermal degradation of the pure PU in dynamic condition shows two distinct decomposition stages. The first stage of decomposition was in temperature region from 278 to 321°C. This stage corresponded to 30 wt % weight loss, which may be caused mainly by the breaking of urethane bond, resulting in the loss of TDI and 1,4-BD moieties.[14] The second decomposition stage, in the temperature range of 363–465°C, was due to the escape of the castor oil molecules and the weight losses reached 56 wt %.[14] The thermogravimetric trace of NGG revealed that decomposition of NGG was a single step degradation process, which decomposition started at 184°C and proceeded at a faster rate up to 198°C. The weight loss reached dramatically 90 wt %, which was resulted from the loss of hydroxyl group of NGG as water molecules and disintegration of molecule chains of NGG.[39] In the PUNG films, there were apparent three weight loss step in the course of thermal degradation: the first step degradation, between nearly 180–200°C, corresponded to the NGG decomposition in blend films, and then the second and third step degradation, between nearly 280–460°C, ascribed to PU degradation.

The slopes of ln[ln $(1/y)$] versus $1/T$ were refined and the activation energies for each major stage of decomposition were evaluated from the slope and listed in Table II. As an example, typical Broido plot for the determination of activation energies for second step weight loss of PU and PUNG films are given in Figure 13. According to the Table II, it can be noted that the total activation energy (E) of thermal decomposition (562.0, 550.3, 546.7, and 633.6 kJ/mol in PUNG-10, PUNG-20, PUNG-40, and PUNG-60 film, respectively) of the PUNG films was higher than that from the pure PU (389.5 kJ/mol) and NGG (372.7 kJ/mol). Furthermore, the residual rate of the PUNG-10, PUNG-20, PUNG-40, and PUNG-60 film (8.7, 12.2, 20.1, and 9.8 wt %) at 500°C was higher than that of the PU film (3.1 wt %) and NGG film (0.8 wt %), which indicated the strong interaction between PU and NGG enhanced the thermal stability of the blend films.

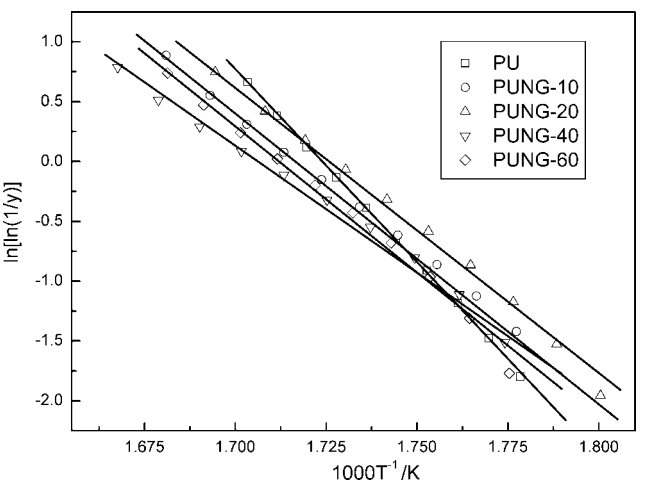

Figure 13 Typical Broido plot for the determination of activation energies for second-step weight loss of the PU and PUNG films.

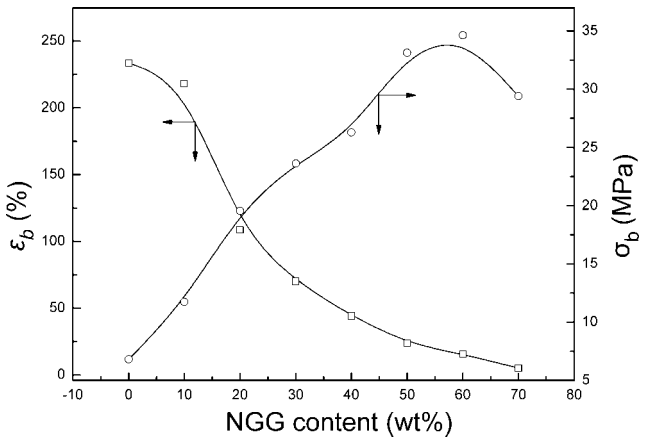

Figure 14 Dependence of tensile strength and breaking elongation on NGG content for the PU and PUNG films.

Mechanical properties of the blend films

The tensile strength (σ and breaking elongation (ε_b) of the PU and PUNG films are shown in Figure 14. The tensile strength of the PUNG films were improved by the addition of NGG and dramatically increased with increasing NGG content. The values of σ_b for the films increased from 11.7 to 28.4 MPa when the NGG content increased from 10 to 70 wt %. However, the breaking elongation of PUNG films sharply decreased with increasing NGG content. NGG is a linear polymer with relatively highly rigid molecular chains, the main chain of which contains two or more —ONO_2 groups per repeating unit, resulting in intermolecular interactions between two components through hydrogen-bonding in the semi-IPNs systems. Obviously, NGG as a strengthening agent mainly played a role in the enhancement of the toughness of the sheets in the blend films.

Solvent-resistance of the blend films

The weight loss rate (W_{loss}) of the pure PU and PUNG films in different solvents including distilled water, 20 wt % HCl solutions, 20 wt % NaOH solutions, 20 wt % NaCl solutions, toluene, and ethanol at room temperature for 7 days are summarized in Table III. Compared with the pure PU film, the PUNG films improved the resistance of solvents including distilled water, alkali solutions, and acid solutions. The weight loss rate remained nearly 0.5–2.0 wt %, which was lower than that of the pure PU. Furthermore, with an increase in NGG content, the weight loss rate of the PUNG films in organic solvents including toluene and ethanol decreased dramatically. Especially, when the NGG content exceeded 40 wt %, the weight loss rate remained at a lower value. The facts indicated that NGG played an important role in enhancement of solvent-resistance for the blend materials.

CONCLUSIONS

New semi-IPNs materials with excellent properties were prepared successfully from a castor oil-based PU prepolymer and NGG with a content of 10–70 wt %. The results from SEM, DSC, DMTA, WAXD, T_r, and density measurement indicated that the PUNG films had good miscibility over the entire composition range under study because of strong intermolecular interactions between the two components. The results from TGA, tensile testing, and solvent resistance test indicated that the NGG played an important role in improving the thermal stability, mechanical properties, and solvent-resistance of the blend films. With an increase in the NGG concentration from 10 to 70 wt %, the tensile strength of the PUNG films increased from 11.7 to 28.4 MPa, which indicated a suitable content of NGG in PUNG films played an important role in the promotion of PU network formation, resulting in the enhancement of strength and toughness. Therefore, we provided a new method for preparing composite materials with excellent mechanical properties from natural polymers.

TABLE III
Resistance of the PU, PUNG Films, and NGG to Some Solvents

	W_{loss}/%					
Samples	Water	20 wt % HCl	20 wt % NaOH	20 wt % NaCl	Toluene	Ethanol
PU	2.52	2.47	2.70	3.29	17.37	21.88
PUNG-10	2.37	1.73	2.49	2.44	15.61	18.02
PUNG-20	1.59	1.58	2.36	1.71	12.17	15.73
PUNG-30	0.64	0.53	1.44	0.45	8.57	13.81
PUNG-40	1.63	0.76	1.35	1.56	7.79	11.61
PUNG-50	1.74	1.16	1.05	0.43	5.42	11.32
PUNG-60	1.32	1.88	1.70	1.61	4.28	7.96
PUNG-70	1.89	1.47	1.52	1.83	4.31	7.08

References

1. Choi, E. J.; Kim, C. H.; Park, J. K. Macromolecules 1999, 32, 7402.
2. Gao, S.; Nishinari, K. Biomacromolecules 2004, 5, 175.
3. Cheng, Y.; Brown, K. M.; Prud'homme, R. K. Biomacromolecules 2002, 3, 456.
4. Wientjes, R. H. W.; Duits, M. H. G.; Jongschaap, R. J. J.; Mellema, J. Macromolecules 2000, 33, 9594.
5. Fox, J. E. In Thickening and Gelling Agents for Food, 2nd ed.; Imeson, A., Ed.; Blackie Academic Professional: New York, 1997; p 262.
6. Brode, G. L.; Goddard, E. D.; Harris, W. C.; Salensky, G. A. In Cosmetic and Pharmaceutical Applications of Polymers; Gebelein, C. G., Cheng, T.C., Yang, V. C., Eds.; Plenum: New York, 1991; p 117.
7. Arvanitoyannis, I. J Macromol Sci Rev Macromol Chem Phys 1999, 39, 205.
8. Coleman, M. M.; Zarian, J. J Polym Sci Polym Phys Ed 1979, 17, 837.
9. Carvalho, A. J. F.; Job, A. E.; Alves, N.; Curvelo, A. A. S.; Gandini, A. Carbohydr Polym 2003, 53, 95.
10. Thomas, D. A.; Sperling, L. H. Polymer Blends, Vol. 2.; Plenum: New York, 1979.
11. Hourston, D. J.; Zia, Y. J Appl Polym Sci 1984, 29, 2963.
12. Gao, S.; Zhang, L. J Appl Polym Sci 2001, 81, 2076.
13. Gao, S.; Zhang, L. Macromolecules 2001, 34, 2202.
14. Zhang, L.; Jin, H. J Appl Polym Sci 2001, 80, 1213.
15. Huang, J.; Zhang, L. Polymer 2002, 43, 2287.
16. Lu, Y.; Zhang, L. Polymer 2002, 43, 3979.
17. Liu, H.; Zhang, L. J Appl Polym Sci 2001, 82, 3109.
18. Zhang, L.; Zhou, Q. Ind Eng Chem Res 1997, 36, 2651.
19. Gong, P.; Zhang, L. J Appl Polym Sci 1998, 68, 1313.
20. Zhang, L.; Zhou, J.; Huang, J.; Gong, P.; Zhou, Q. Ind Eng Chem Res 1999, 38, 4684.
21. Lu, Y.; Zhang, L. Ind Eng Chem Res 2002, 41, 1234.
22. Trivedi, H. C.; Patel, C. K.; Patel, R. D. Angew Macromol Chem 1978, 70, 39.
23. Joshi, K. M.; Sinha, V. K.; Patel, C. P.; Trivedi, H. C. Macromol Rep 1995, A-32,133.
24. Williams, D. H.; Fleming, I. Spectroscopic Methods on Organic Chemistry, 3rd ed.; McGraw-Hill: London, 1980; p 44.
25. Devia, N.; Manson, J. A.; Sperling, L. H.; Conde, A. Macromolecules 1979, 12, 360.
26. Broido, A. J Polym Sci Part A-1: Polym Chem 1969, 27, 1761.
27. Zhang, L.; Huang, J. J Appl Polym Sci 2001, 81, 3251.
28. Coleman, M. M.; Lee, K. H.; Skrovanek, D. J.; Painter, P. C. Macromolecules 1986, 19, 2149.
29. Miller, J. A.; Lin, S. B.; Hwang, K. K. S.; Wu, K. S.; Gibson, P. E.; Cooper, S. L. Macromolecules 1985, 18, 32.
30. Paik, S. C.; Smith, T. W.; Sung, N. H. Macromolecules 1980, 13, 117.
31. Queiroz, D. P.; Pinho, M. N.; Dias, C. Macromolecules 2003, 36, 4195.
32. Velanker, S.; Cooper, S. L. Macromolecules 2000, 33, 382.
33. Roland, C. M.; Ngai, K. L. Prog Colloid Polym Sci 1993, 91, 75.
34. Klempner, D.; Frisch, H. L. J Polym Sci Part B: Polym Lett 1970, 8, 525.
35. Martin, D. J.; Meijs, G. F.; Renwick, G. M.; Gunatillake, P. A.; McCarthy, S. J. J Appl Polym Sci 1996, 60, 557.
36. Chen, Y.; Zhang, L.; Du, L. B. Ind Eng Chem Res 2003, 42, 6786.
37. Krause, S. J Macromol Sci Rev Macromol Chem 1972, 7, 251.
38. Yang, J.; Winnik, M. A.; Ylitalo, D.; Devoe, R. J. Maromolecules 1996, 29, 7047.
39. Soppirnath, K. S.; Aminabhavi, T. M. Eur J Pharm Biopharm 2002, 53, 87.